Int. J. Heat Mass Transfer. Vol. 36, No. 9, pp. 2449–2456, 1993
Printed in Great Britain

0017-9310/93 $6.00+0.00
Pergamon Press Ltd

Thermal processes in gas–powder laser cladding of metal materials

V. K. PUSTOVALOV and D. S. BOBUCHENKO
Byelorussian State Polytechnic Academy, Minsk, 220027, Belarus

(*Received* 9 *January* 1992)

Abstract—Energy absorption, heating, melting and heat transfer in a gas–powder laser cladding of substrate metal powders are theoretically investigated. A system of equations is formulated which describes optical and thermal processes of the gas–powder laser cladding. Based on the numerical solution of the system of equations formulated, spatial temporal temperature distributions in one-dimensional approximation and time dependences of the process parameters for continuous and pulse cladding modes are obtained. A possibility is demonstrated to melt metal particles in the laser radiation beam prior to their getting to the surface, which could lead to enhancing the cladding process efficiency and upgrading the cladded layer. Some specific features of the pulse mode of the powdered material cladding are studied.

1. INTRODUCTION

PRESENTLY, one of the pressing problems of modern engineering is the production of special and durable coatings on surfaces of various elements. A cladding of powdered metal materials onto the element sections is an efficient technological process resulting in a strengthening and increase of durability of heavy-loaded elements of internal-combustion engines, machines, power-generating plants, etc. Moreover, the powdered material cladding is widely used in repairing and reconstructing worn-out and destroyed sections of elements. Recently, extensive experimental investigations have been performed, and various modes and methods of cladding powdered metal materials by intense laser radiation have been proposed [1–3]. At the same time, studies on numerical simulation of the gas–powder cladding are actually absent. Mazumder and Kar [4] have undertaken an effort to predict one-dimensional thermal characteristics in the laser powder cladding. However, this work lacks a consideration of moving powder particles proper and of their interaction with laser radiation prior to getting to the built-up layer surface. In connection with the foregoing, it is of great interest to investigate the gas–powder laser cladding taking account of the thermal processes of the radiation interaction with moving dispersed particles, which is effected in the current study. Besides, it is interesting to investigate the effect of initial parameters on the laser cladding process in order to optimize and substantiate existing modes and methods and to search for novel ones.

The current study has formulated a physico-mathematical model and presents results of numerically simulating some modes of the gas–powder laser cladding of metal materials onto an immovable substrate.

2. MATHEMATICAL STATEMENT OF THE PROBLEM

The gas–powder laser cladding (GPLC) consists in producing surface coatings of powdered materials on elements (substrates) with the aid of the laser radiation beam. In this case, there occurs a partial melting of the element surface by radiation, a powder (dispersed metal particles) feeding to the laser irradiation zone by a gas flow, a heating of the particles by radiation, their reaching the molten surface, an intermixing and a diffusional interpenetration of the particle and substrate materials, and a cooling (crystallization) of the coating formed [1–3].

Let a physicomathematical model of the gas–powder cladding be formulated. Consider a propagation of intense radiation of the wavelength λ along the axis X, with the beam axis coinciding with the axis X of the cylindrical coordinate system X, R. The metal surface substrate is positioned normal to the axis X at the point $X = X_3$ (see Fig. 1). Let, in the section

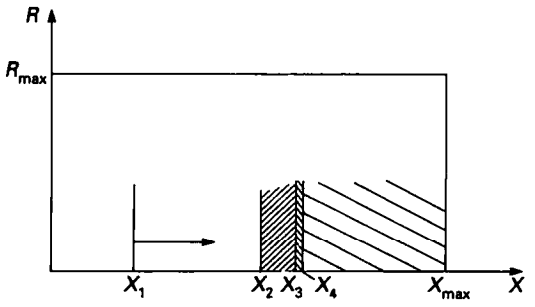

FIG. 1. A geometric model of the cladding process; X_2-X_1, the region of irradiation of moving particles (an arrow indicates a direction of the radiation propagation and particle movement); X_3-X_2, a cladded material; X_4-X_3, a molten substrate material; $X > X_4$, a solid substrate material.

NOMENCLATURE

A_{ab}	absorptivity of condensed phase
c	specific heat
c_0	specific heat of particle material
c_m	specific heat of gas medium
c_1	specific heat of vapour
c_2	specific heat of inert gas
D	vapour diffusivity in gas
E	heat energy of particles
f_0	function of particle radius distribution
I	radiation intensity
j_m	density of mass flux from particle
j_ε	density of energy flux from particle
j_h	energy flux density removed by heat conduction
K_{ab}	efficiency of radiation absorption by particle
K_{sc}	efficiency of radiation scattering by particle
K_a	efficiency of radiation attenuation by particle
L_{ev}	specific heat of evaporation
L_{mel}	specific heat of melting
N_0	particle concentration
P	pressure
Q	integral values of energies characterizing the process of radiation interaction with particle
r_0	particle radius
R	radial coordinate in the cylindrical coordinate system
R_g	gas constant
T	temperature
T_c	condensed phase temperature
T_0	particle temperature
T_m	gas medium temperature
T_{mel}	melting temperature
t	time
t_{in}	initial time instant of powder cladding onto substrate
t_p	duration of radiation pulse
u	gas flow velocity
$\bar{v}_x$	particle velocity
X	coordinate.

Greek symbols

α_T	coefficient of convective heat transfer
α_{a0}	coefficient of radiation attenuation by particles
α_{ah}	coefficient of radiation attenuation by heat and mass haloes
α_{am}	coefficient of radiation attenuation by gas phase
ε	surface blackness
η	dynamic viscosity
λ	radiation wavelength
κ	thermal conductivity
ρ_0	density of particle material
ρ_m	density of vapour–gas medium
ρ_1	vapour density of particle material
ρ_2	density of inert gas
σ	Stefan–Boltzmann constant.

Subscripts

ab	absorption
sc	scattering
mel	melting
h	heat conduction
rad	radiative cooling
max	maximum value
m	gas medium
∞	initial value.

$X_1 < X_3$, the dispersed particles with the initial concentration N_0, radii r_∞, temperature T_∞ and function of the particle size distribution $f_\infty(r_\infty)$ be introduced into the radiation beam by the gas flow. The particles move in the radiation beam along the axis A, absorb and scatter its energy, get heated and arrive at the substrate surface. Radiation is absorbed and reflected by the metal substrate surface; here, when the intensity is sufficient, the surface substrate layer melts. Upon the powder particle reaching the molten surface substrate layer, a deposition and growth of the cladded powder layer occur. The metal particles move in the inert gas flow at atmospheric pressure, i.e. the processes of oxidation, ignition and combustion of the metal particles and metal substrate surface [5, 6] by radiation can be disregarded.

Consider the GPLC under the action of radiation of duration t_p, when the temperature inside the particles and the gas pressure (with allowance for certain gas temperature and vapour density distributions) within the radiation beam can be assumed equalized and the particle heat exchange with the surrounding gas can be analyzed in a quasi-steady approximation. Those approximations have been discussed and substantiated in ref. [7]. It must be noted that consideration is given to the cladding modes with the duration t_p satisfying the aforementioned conditions. In the given case, a system of equations describing the processes of laser cladding of the dispersed metal particles, moving in the inert gas flow, onto the immovable metal substrate has the form [7]

$$\frac{\partial I}{\partial X} + (\alpha_{a0} + \alpha_{ah} + \alpha_{am}) = 0 \qquad (1)$$

$$\rho_0 V_0 c_0 \left(\frac{\partial T_0}{\partial t} + (v_x \nabla) T_0\right) = \tfrac{1}{4} I K_{ab} S_0 - \bar{j}_\varepsilon S_0 \quad (2)$$

$$\frac{\partial(\rho_0 V_0)}{\partial t} + (v_x \nabla)(\rho_0 v_0) = -\bar{j}_m S_0 \quad (3)$$

$$\frac{\partial f_0}{\partial t} + (v_x \nabla) f_0 + \frac{\partial}{\partial r_0}\left(f_0 \frac{\partial r_0}{\partial t}\right) = 0 \quad (4)$$

$$\rho_0 V_0 \left(\frac{\partial v_x}{\partial t} + (v_x \nabla) v_x\right) = 6\pi\eta r_0 (v_x - u) \quad (5)$$

$$\rho_m c_m \left(\frac{\partial T_m}{\partial t} + (u\nabla) T_m\right) = \frac{\partial}{\partial X}\left(\kappa_m \frac{\partial T_m}{\partial X}\right) + \frac{1}{R}\frac{\partial}{\partial R}\left(\kappa_m R \frac{\partial T_m}{\partial R}\right) + q_T \quad (6)$$

$$\frac{\partial \rho_1}{\partial t} + (u\nabla)\rho_1 = \frac{\partial}{\partial X}\left(D_m \rho_m \frac{\partial(\rho_1/\rho_m)}{\partial X}\right) + \frac{1}{R}\frac{\partial}{\partial R}\left(D_m R \rho_m \frac{\partial(\rho_1/\rho_m)}{\partial R}\right) + q_m \quad (7)$$

$$P_m = R_g \rho_m T_m = P_\infty \quad (8)$$

$$\rho_c c_c \frac{\partial T_c}{\partial t} = \frac{\partial}{\partial X}\left(\kappa_c \frac{\partial T_c}{\partial X}\right) + \frac{1}{R}\frac{\partial}{\partial R}\left(\kappa_c R \frac{\partial T_c}{\partial R}\right) \quad (9)$$

with the following initial conditions

$$T_0(X, R, t=0) = T_\infty \quad T_m(X, R, t=0) = T_\infty$$
$$T_c(X, R, t=0) = T_\infty \quad r_0(X, R, t=0) = r_\infty$$
$$\rho_1(X, R, t=0) = 0 \quad \rho_2(X, R, t=0) = \rho_{2\infty}$$
$$f_0(X, R, t=0, r_0) = f_\infty(r_\infty) \quad (10)$$

and boundary conditions

$$T_0(X = X_1, R, t) = T_m(X = X_1, R, t) = T_c(X_{max}, R, t) = T_\infty,$$
$$T_c|_{x_3-0} = T_c|_{x_3+0}, \quad T_c|_{x_4-0} = T_c|_{x_4+0} = T_{mel}$$
$$\kappa_m \frac{\partial T_m}{\partial R}\bigg|_{R=0} = 0; \quad \kappa_c \frac{\partial T_c}{\partial R}\bigg|_{R=0} = 0;$$
$$\rho_m D_m \frac{\partial(\rho_1/\rho_m)}{\partial R}\bigg|_{R=0} = 0;$$
$$I(X = X_1, R = 0, t) = I_0$$
$$T_m(X < X_2, R = R_{max}, t) = T_c(X \geqslant X_2, R = R_{max}, t) = T_\infty;$$
$$\rho_1(X, R = R_{max}, t) = 0$$
$$-\kappa_c \frac{\partial T_c}{\partial X}\bigg|_{x_3-0} = -\kappa_c \frac{\partial T_c}{\partial x}\bigg|_{x_3+0};$$
$$-\kappa_c \frac{\partial T_c}{\partial X}\bigg|_{x_4-0} = -\kappa_c \frac{\partial T_c}{\partial X}\bigg|_{x_4+0} + L_{mel}\rho_c \frac{dX_4}{dt} \quad (11)$$

$$\left[A_{ab} I + N_0 \rho_0 v_x \int_0^\infty (c_0(T_0 - T_c) + L_{mel}) \tfrac{4}{3}\pi r_0^3 f_0 \, dr_0 - \alpha_T (T_m - T_c) - \varepsilon\delta(T_c^4 - T_\infty^4)\right] = -\kappa_c \frac{\partial T_c}{\partial X}\bigg|_{x_2+0}$$

$$0 \leqslant t < t_{in}; \quad X_2 = X_3; \quad t \geqslant t_{in};$$
$$X_2 = X_3 - \frac{w_0 v_x (t - t_{in})}{\rho_0}$$

where I is the radiation intensity;

$$\alpha_{a0} = \pi N_0 \int_0^\infty r_0^2 (K_{ab} + K_{sc}) f_0 \, dr_0,$$

α_{ah}, α_{am} are the coefficients of radiation attenuation by the particles, heat and mass haloes, and gas phase; here α_{ah}, $\alpha_{am} \ll \alpha_{a0}$ and they are neglected; K_{ab}, K_{sc}, $K_a = K_{ab} + K_{sc}$ are, correspondingly, the efficiency factors of the radiation absorption, scattering and attenuation by a particle of the running radius r_0; f_0 is the function of the particle size distribution;

$$\int_0^\infty f_0(r_0) \, dr_0 = 1;$$

ρ_0, and c_0 are, correspondingly, the density and specific heat of the particle material; T_0 is the particle temperature assumed to be uniform over the particle volume; t is the time; $V_0 = \frac{4}{3}\pi r_0^3$; $S_0 = 4\pi r_0^2$; $\bar{j}_m$, and $\bar{j}_\varepsilon$ are, correspondingly, the densities of mass and energy fluxes from the particle surface taking into account the particle heat and mass exchange with gas [8], v_x is the particle velocity along the axis X, η is the dynamic viscosity, $\rho = \rho_1 + \rho_2$, ρ_1 and ρ_2 are, correspondingly, the densities of the vapour–gas medium, particle material vapour and inert gas; κ_m and D are the thermal conductivity of the medium and the vapour diffusivity in the medium; u is the gas flow velocity, T_m is the medium temperature,

$$q_T = 4\pi N_0 \int_0^\infty (\bar{j}_h + \bar{j}_m c_1 (\bar{T} - T_m)) r_0^2 f_0 \, dr_0$$

is the power density of heat release in the medium due to the heat conduction from the particles $\bar{j}_h$ and due to heating by a hot vapour; c_m and c_1, c_2 are the specific heat of the vapour–gas medium, vapour and gas, respectively; $\bar{T}$ is the medium temperature directly at the particle surfaces;

$$q_m = 4\pi N_0 \int_0^\infty \bar{j}_m r_0^2 f_0 \, dr_0$$

is the power density of vapour generation in the medium due to the particle evaporation; P_m is the pressure, R_g is the gas constant; r_∞, $\rho_{2\infty}$, f_∞, T_∞ and P_∞ are the initial values of relevant parameters;

$$\bar{j}_\varepsilon = \bar{j}_h + \bar{j}_m (c_1 (\bar{T} - T_m) + L_{ev}) + \bar{j}_{rad};$$

L_{ev} is the specific evaporation heat of the particle material, $\bar{j}_{rad} = \varepsilon\sigma(T_0^4 - T_\infty^4)$ is the energy flux density

removed from the particle by heat radiation; ε is the blackness of the particle surface; σ is the Stefan–Boltzmann constant;

$$w_0 = \tfrac{4}{3}\pi N_0 \int_0^\infty r_0^3 f_0 \, \mathrm{d}r_0$$

is the particle material mass per unit volume of the medium; the radius R_{max} and the length X_{max} of the calculated volume are chosen such that unperturbed initial parameters on its boundaries be retained in the time interval under consideration; t_{in} is the initial time instant of the powder cladding onto the substrate; ρ_c, c_c and κ_c are, correspondingly, the density, specific heat and thermal conductivity of the condensed phase for $X > X_2(X_3)$ with allowance for the difference in these magnitudes for the cladded material and starting substrate material; T_c is the condensed phase temperature; L_{mel} is the specific heat of melting, α_T is the convective heat transfer coefficient; A_{ab} is the absorptivity of the condensed phase surface.

The system of equations (1)–(9) involves the quasi-stationary radiation transfer equation (1) in the approximation of single radiation scattering on the particles, equations of energy (2) and mass (3) balance for individual moving particles, equations (4) describing a variation in the function of the particle size distribution resulting from evaporation; equations of particle movement in the gas flow (5); two-dimensional equations of the gas medium heat conduction (6) and of vapour diffusion (7); equation of state of the vapour–gas medium (8) and heat conduction equation for the condensed phase (for the cladded material and substrate material) (9). In the boundary conditions (11) on the surface X_2 separating the condensed phase and the oncoming two-phase medium, the energy flux conservation law is fulfilled with regard to radiation energy absorption by the surface, heat energy transfer of the surface particles, the surface heat transfer by convective heat exchange and radiative cooling and heat removal deep into the condensed phase. The motion equation for X_2 is based on a fulfillment of the mass conservation law for the cladded particles. Here, no account is taken of evaporation from the condensed phase surface. On the boundary X_3 between the cladded material and the substrate material, the heat flux continuity is achieved. On the boundary X_4 between the solid and molten material, the heat flux conservation law with allowance for energy consumption on melting is fulfilled. At various stages of the process, $X_4 \gtrless X_3$ is possible.

A numerical solution of the formulated system of equations (1)–(9) taking account of equations (10)–(12) is an extremely difficult task even with modern computers and is dependent on the required operation speed (in this case quick), storage volume, etc. On the other hand, there is no need for a too detailed description of the gas–powder laser build up, inasmuch as the basic regularities and salient features of the process can be ascertained from the numerical solution of a simplified system of equations, which will be formulated using the results of experimental investigation of the powder laser cladding [1–3]. Let us restrict ourselves to the values of the radiation intensity I_0 at which a heating and melting of the particles of the powder and surface substrate layer can occur, but their evaporation is virtually absent. Since the metal evaporation is intense at a temperature $T \geqslant T_b$, where T_b is the boiling temperature of the metal at atmospheric pressure, the modes without particle and substrate evaporation can always be realized over the considerable temperature range $T_{mel} \leqslant T < T_b$. Obviously, exactly such modes which do not bring about a decrease in the cladded material mass due to evaporation are of practical interest. In this case, equations (3), (4) and (7) drop out of the system (1)–(9) and, in $\bar{j}_e$, q_T, the mass flux density is $\bar{j}_m = 0$, i.e. the particles and substrate surface only exchange heat with the ambience. Let the particle velocity v_x equal the gas velocity u, which allows equation (5) not to be considered. Also we will confine ourselves to examining one-dimensional equations (1), (2), (6) and (9) along the axis X, since the gradients of quantities along X are much in excess of the corresponding gradients along R, and the treatment of a cladded layer growth along X on the beam axis is of the greatest practical importance. Thus, the system of one-dimensional, along X, equations (1), (2), (6), (8) and (9) is solved numerically in view of equations (10) and (11). Here, use is made of a multigroup approximation for the initial function of the particle size distribution $f_\infty(r_\infty)$ and equation (2) is solved individually for each group of particles with the proper r_∞. Moreover, the radiation energies $Q_{ab}(r_\infty, X, t)$ and $Q_{sc}(r_\infty, X, t)$, (correspondingly, absorbed and scattered by the particle) as well as $Q_{mel}(r_\infty, X, t)$, $Q_h(r_\infty, X, t)$, $Q_{rad}(r_\infty, X, t)$ (correspondingly, expended on melting and removed from the particle by heat conduction and radiative cooling) are predicted for a particle passing at the time instant $t \geqslant 0$ through the section x_1

$$Q_{ab} = \pi r_\infty^2 \int_t^{t_y+t} IK_{ab}(r_\infty)\,\mathrm{d}t$$

$$Q_{sc} = \pi r_\infty^2 \int_t^{t_y+t} K_{sc}(r_\infty) I\,\mathrm{d}t$$

$$Q_{mel} = \rho_0 V_0 L_{mel} \quad Q_h = 4\pi r_\infty^2 \int_t^{t_y+t} \bar{j}_h\,\mathrm{d}t$$

$$Q_{rad} = 4\pi r_\infty^2 \int_t^{t_y+t} \bar{j}_{rad}\,\mathrm{d}t \qquad (12)$$

where $t_y = (X_2 - X_1)/\bar{v}_x$ is the travel time of the particle exposed to radiation with the particle coordinate X varying within $X_1 \leqslant X \leqslant X_2$.

When the particle travels over the spatial region $X_1 \leqslant X \leqslant X_2$, the energy conservation law for each

particle, calculated over the range from t to $t+t_y$, is fulfilled

$$Q_{ab}+E_\infty = Q_h+Q_{rad}+Q_{mel}+E \tag{13}$$

where

$$E=\int_0^{T_0}\rho_0 V_0 c_0\,\mathrm{d}T_0$$

is the particle heat energy and $E_\infty = E(T_\infty)$. Besides, the energy density conservation laws are computed from the time instant $t=0$ up to a given time instant t for the radiation–particles–substrate system in question which have the form

$$S_r = S_{ab}+S_{sc}+S_{abc}+S_{rc} \tag{14}$$

$$S_{ab} = S_{rad}+S_{T0}+S_{y0}-S_\infty \tag{15}$$

$$S_{abc}+S_{y1} = S_{radc}+S_{hc}+S_{melc}+S_{Tc}-S_{Tc\infty} \tag{16}$$

where $S_r=\int_0^t I_0\,\mathrm{d}t$ is the energy density of laser radiation which passed through X_1;

$$S_{ab}=N_0 v_x\int_0^t\int_0^\infty Q_{ab}\,f_\infty(r_\infty)\,\mathrm{d}r_\infty\,\mathrm{d}t,$$

and

$$S_{sc}=N_0 v_x\int_0^t\int_0^\infty Q_{sc} f_\infty(r_\infty)\,\mathrm{d}r_\infty\,\mathrm{d}t$$

are, accordingly, the densities of radiation energy absorbed and scattered by the particles moving from X_1 to X_2 and

$$S_{abc}=\int_0^t I(X_2)A_{ab}\,\mathrm{d}t$$

and

$$S_{rc}=\int_0^t I(X_2)(1-A_{ab})\,\mathrm{d}t$$

are, accordingly, the densities of radiation energies absorbed and reflected by the condensed phase surface at $X_2(X_3)$,

$$S_y=N_0 v_x\int_0^t\int_0^\infty (E+\rho_0 V_\infty L_{mel})f_\infty(r_\infty)\,\mathrm{d}r_\infty\,\mathrm{d}t,$$

$$S_{y0}=S_y(t=0),$$

$S_{y1}=S_y(t=t_p)$ is the density of energy brought by the particle to the condensed phase surface;

$$S_{rad}=N_0 v_x\int_0^t\int_0^\infty Q_{rad}\,f_\infty(r_\infty)\,\mathrm{d}r_\infty\,\mathrm{d}t$$

and

$$S_{T0}=N_0 v_x\int_0^t\int_0^\infty Q_h\,f_\infty(r_\infty)\,\mathrm{d}r_\infty\,\mathrm{d}t$$

are, accordingly, the densities of energies removed from the particle surface by radiative cooling and heat conduction,

$$S_{T\infty}=N_0 v_x\int_0^L\int_0^\infty E_\infty f_\infty(r_\infty)\,\mathrm{d}r_\infty\,\mathrm{d}t,$$

$$S_{hc}=\int_0^t \alpha_T(T_c-T_m)|_{x2}\,\mathrm{d}t$$

and

$$S_{radc}=\int_0^t \varepsilon\delta(T_c^4-T_m^4)|_{x2}\,\mathrm{d}t$$

are, accordingly, the densities of energies removed from the surface by convective and radiative heat transfer,

$$S_{Tc}-S_{Tc\infty}=\int_{x_2}^\infty \rho_c c_c(T_c-T_\infty)\,\mathrm{d}X$$

and

$$S_{melc}=\rho_c(X_4-X_5)L_{mel}$$

for $X_4\geqslant X_3$ are, accordingly, the densities of heat energy expended on melting the substrate metal.

Relation (14) indicates that radiation energy is absorbed and scattered by the moving particles, and is also absorbed and reflected by the condensed phase surface. The energy density absorbed by the particles S_{ab} (15) is spent on heating and melting the particles and, with the deduction of heat loss by radiative cooling and heat conduction, is transferred from the particles to the surface X_2, when $t>t_{in}$. The density of energies absorbed by the surface S_{abc} and transported by the particles to the surface S_{y1} (16) is expended on heating and melting the substrate metal, and is also removed from the surface by convective and radiative heat transfer.

Furthermore, energy parameters characterizing the GPLC process are computed

$$H_1=\frac{S_{ab}+S_{abc}}{S_r};\quad H_2=\frac{S_{abc}}{S_{abc}+S_{rc}};\quad H_3=\frac{S_{ab}}{S_{ab}+S_{sc}}$$

$$H_4=\frac{S_{y0}-S_{T\infty}}{S_{ab}};\quad H_5=\frac{S_{melc}+S_{Tc}-S_{Tc\infty}}{S_{abc}+S_{y1}} \tag{17}$$

where H_1 characterizes the contribution of radiation energy absorption by the particles and surface and represents the process efficiency; H_2 and H_3 define, correspondingly, the contribution of radiation energy absorption by the surface and particles relative to absorption and reflection by the surface and to absorption and scattering by the particles. The parameters H_4 and H_5 specify the ratio of energy density consumed on heating and melting the particles and surface to energy density absorbed by the particles and that absorbed by the surface and transferred by the particles to the surface during the cladding process. Energy integrals (12)–(16) are calculated via the trapezoidal rule with an error not larger than 1%, which is evidence of sufficient accuracy of the numerical calculation (1), (2), (6) and (9).

3. RESULTS OF NUMERICAL CALCULATION

Consider some results of numerical calculations for the process of aluminum powder cladding onto a steel substrate by intense laser radiation of the wavelength $\lambda = 10.6$ μm. The aluminum particle dispersivity is taken into account in the multigroup approximation and use is made of the following initial radii $r_{\infty i} = 15$, 20, 25, 30 and 35 μm and weights, $f_{\infty i} = 0.1$, 0.2, 0.4, 0.2 and 0.1 of the particle groups. The aluminum particles move in a helium flow, with the velocity $v_x = 20$ m s^{-1} at atmospheric pressure, the interval on which the particles interact with radiation being equal to $X_3 - X_1 = 1$ cm. The particle concentration N_0 is $N_0 = 1.5 \times 10^4$ cm^{-3} and the initial gas, particle and substrate temperature is $T_\infty = 300$ K. Radiation intensity is unchangeable in time and equal to $I_0 = 400$ kW cm^{-2}. The values of physical characteristics of aluminum, iron and helium are borrowed from refs. [9–11].

To enhance the absorptivity A of the substrate metal, it is treated in an appropriate manner with increasing roughness degree or coated with a special high-absorptivity paint [2]. Moreover, during the powder cladding onto the substrate, the surface being formed is also rough. In this case, scattered radiation reflection from the surface occurs which permits a disregard of the effect of back-scattered radiation on the particles moving towards the surface. The absorptivity A_{ab} of metal increases stepwise upon its melting [12–14]. Here, in view of the foregoing for the dependence of A_{ab} on the temperature T, the following empirical relation is employed [12–14]:

$$A_{ab} = A_{ab\infty} + A_{ab1}(T_c - T_\infty), \quad T_\infty \leqslant T_c < T_{mel};$$
$$A_{ab} = A_{ab2}, \quad T_c \geqslant T_{mel}; \qquad (18)$$

where $A_{ab\infty}$, A_{ab1} and A_{ab2} are the constants and T_{mel} is the melting temperature. At $\lambda = 10.6$ μm, use was made of $A_{ab\infty} = 0.12$, $A_{ab1} = 2.65 \times 10^{-5}$ K^{-1} and $A_{ab2} = 0.6$ for iron [12, 14] and of $A_{ab\infty} = 4.2 \times 10^{-2}$, $A_{ab1} = 1.43 \times 10^{-5}$ K^{-1} and $A_{ab2} = 7.1 \times 10^{-2}$ for aluminum [15].

Consider the intense radiation effects on metal powder particles moving from X_1 to $X_3(X_2)$. The time the particle travels, starting from the instant of irradiation onset, from the boundary X_1 to the surface X_3 (in the process of cladding to X_2) is virtually the setting time t_y of a stationary distribution of the two-phase medium (particles and gas) parameters along X in the spatial interval $X_3 - X_1$. In the given case, t_y comprises $t_y = (X_2 - X_1)/v_x = 5 \times 10^{-4}$ s. For $t < t_y$, the particle irradiation process is unsteady, whereas, for $t \geqslant t_y$, it is steady. Figure 2 gives the distributions of temperatures of the particles with $r_\infty = 15$, 25 and 35 μm and of the normalized radiation intensity $I_{in} = I/I_0$ for several time instants along X in the range $X_3 - X_1$. From the initial time instant of the moving particle irradiation, there begins radiation energy absorption and the particle heating as well as radiation scattering and attenuation by the particles. Here,

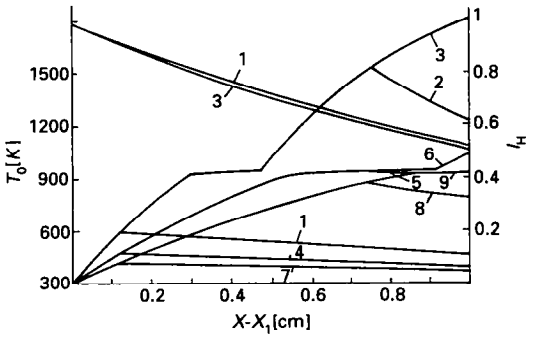

FIG. 2. Distributions of the temperature T_0 (———) of particles with $r_\infty = 15$ (1–3), 25 (4–6), and 35 (7–9) μm, of the normalized radiation intensity I (1, 3) for the time instants $t = 6.21 \times 10^{-5}$ (1, 4, 7), 3.74×10^{-4} (2, 5, 8), 5×10^{-4} (3, 6, 9) s along X in the interval $X_3 - X_1$.

the particle somewhat screens the substrate surface and, as the particle moves from X_1 to the surface, it is exposed to radiation of diminishing intensity. On the given particle temperature reaching the melting temperature T_{mel}, the moving particles melt over a certain period of time thus giving rise to a 'step' in the distribution of T_0 along X (see Fig. 2). With the particle moving from X_1 to X_3, its temperature rises. At a time instant $t < t_y$, the particles at the point $X = X_1 + v_x t$ have a maximum temperature for a given r_∞, whereas at the time instant $t = 0$, the temperature of the particles at the point X_1 is maximum. When $t > t_y$, the particle temperature is maximum for $X = X_3(X_2)$. Here, the particle heating rate is higher for smaller r_∞, since in this case heat removal from the particles is much less than their energy release. Inasmuch as the radius of the particles increases with their melting due to irradiation, [6, 8], the radiation attenuation by the particles somewhat increases for $t > t_y$ (see Fig. 2). Thus, based on the numerical simulation, the possibility is established of the metal particle melting in the radiation beam before the particle gets to the substrate surface (see ref. [3]). This can improve efficiency of the cladding process and upgrade the cladded layer. It should also be noted that the increase in the medium temperature ΔT_m for $X \leqslant X_3(X_2)$ in consequence of heat exchange of the heated particles with the surrounding gas is, in this case, not larger than $\Delta T_m = T_m - T_\infty < 1$–2 K.

Figure 3 presents the distribution of the condensed phase temperature T_c over X for $X > X_2$ and for several time instants. From the instant of radiation incidence onto the substrate surface, its heating and temperature growth are accompanied by heat exchange with the moving gas and by heat removal deep into the substrate.

Once the melting temperature is reached, the surface substrate layer melts and the melting front propagated deep into the substrate. It was assumed that, prior to the substrate melting and to the formation of a melting bath of a definite depth, for example,

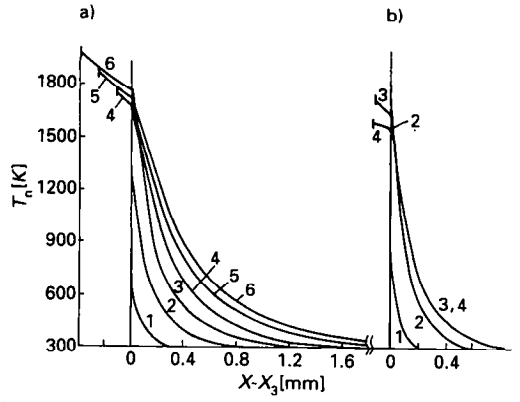

FIG. 3. A distribution of the temperature T_c at $t = 5 \times 10^{-4}$ (1), 3×10^{-3} (2), 6×10^{-3} (3), 1.11×10^{-2} (4), 1.71×10^{-2} (5), 2.31×10^{-2} (6) s (a) and $t = 2 \times 10^{-4}$ (1), 1.79×10^{-3} (2), 3×10^{-3} (3), 3.15×10^{-3} (4) s (b) along X for $X \geqslant X_2$ (a vertical mark denotes the coordinate X_2 at a given time instant).

$X_4 - X_3 \approx 15$ μm, no powder cladding onto the substrate occurs. After the condition of the cladding initiation is fulfilled, the powder cladding onto the substrate proceeds from the time instant t_{in}, with temperature rising with a decrease of X in the built-up layer. It must be pointed out that a lifetime of the molten substrate metal layer is, in this case, short and equal to 6×10^{-4} s, the effect of the substrate step A_{ab} being also insignificant in melting.

Figure 4 gives time dependences of the cladding parameters H_i ($i = 1$–5) and of the coordinates of the melting front X_4 and of the cladded material surface X_2. The melting front X_4 departs from the substrate surface at a depth of about 15 μm; thereafter the cladding condition is realized and the melting front returns to the point X_3 and retains this position over the calculated time interval. A problem is that the aluminum melting temperature of 933.6 K is appreciably lower than the iron melting temperature of 1810 K [11]. Here, in the cladding process, the cladded aluminum layer is in a molten state, whereas the substrate is in a solid state. From the instant of realization of the cladding condition, the cladded layer thickness

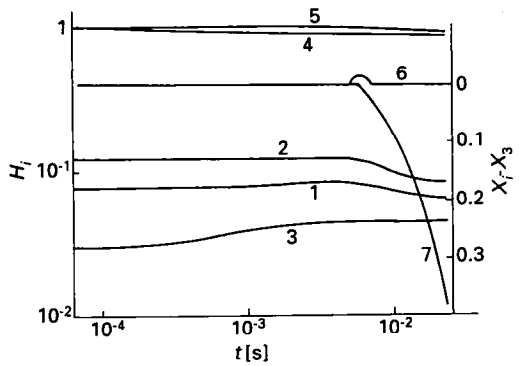

FIG. 4. The parameters H_i, $i = 1$–5 (1–5) and the coordinates of the melting front X_4 (6) and of the cladded material surface X_2 (7) as functions of the time t.

starts growing rapidly. In this case, the thickness $X_3 - X_2 = \bar{w}_\infty v_x (t - t_{in})/\rho_0$ for $t > t_{in}$ increases uniformly with time.

From the initial instant of the cladding, the parameter H_1 decreases with time, since energy absorption on the condensed phase surface decreases as a result of the iron replacement by aluminum. It should be noted that the cladding efficiency is here $H_1 \leqslant 0.1$, which is due to a marked scattering of radiation energy by the particles and to a condensed phase reflection by the surface. The parameter H_2 behaves in a similar fashion. The parameter H_3 increases to some extent owing to a nonlinear increase in the radiation energy absorption by the aluminum particles during heating and melting [6, 8]. In the given case, energy losses by heat exchange and radiative cooling of the particles and substrate are small and H_4, $H_5 \geqslant 0.92$–0.96.

In connection with the development and application of pulse and pulse–periodic lasers, it is of great scientific and practical interest to study appropriate cladding modes with radiation to the lasers used, as well as distinctive features and differences of these modes from the mode of cladding by continuous radiation. A numerical calculation was performed for a pulse cladding version with the pulse duration $t_p = 3 \times 10^{-3}$ s, $I_0 = 1.2$ MW cm^{-2}, particle concentration $N_0 = 2.5 \times 10^4$ cm^{-3} and particle velocity $v_x = 50$ m s^{-1}. Since the particle and substrate irradiation time and, correspondingly, the cladding time in this case decrease, in order to produce, during the pulse, a noticeable thickness of the cladded material layer it is necessary to employ I_0, N_0, and v_x values larger than those in the case of a continuous cladding. The rest of the parameters are taken to be the same as in the previous version.

The behaviour of the particles moving to the condensed phase surface in the laser irradiation beam during the pulse is analogous to the behaviour of the moving particles from the initial time instant of the continuous radiation. Over the time t of travel from X_1 to X_3 (X_2) (in this case, $t = 2 \times 10^{-4}$ s), by the action of radiation the particles manage to melt and acquire the temperature $T_0 \sim 940$–1800 K, correspondingly, for $r_\infty = 35$–15 μm before getting to the surface. Consequently, the powder particles can also be melted by radiation prior to their getting to the substrate (the condensed phase surface) with the pulse cladding mode used.

At the pulse cladding, the temperature distribution in the condensed phase (the substrate) differs appreciably from the previous $T(X)$ distribution (see Figs. 3(a) and (b)). A reduction of the irradiation duration results in a marked decrease of the heated layer thickness. In the given case, the thickness of the substrate material layer heated to the temperature $T \geqslant 10^3$ K comprises about 350 and 120 μm for continuous and pulse modes, respectively. Therefore, using pulse radiation can notably decrease the thickness of the thermal heating zone of the substrate material (the ther-

mal effect). The cladding is initiated at the time instant $t_{in} = 1.8 \times 10^{-3}$ s and, for the time interval $t_p - t_{in} = 1.2 \times 10^{-3}$ s, the cladded layer thickness reaches about 110 μm. Since the molten layer cooling and crystallization after the irradiation termination proceed relatively slowly, the growth of the cladded layer thickness on the powder supply occures for a certain time period after radiation is switched off and ultimately the cladded layer thickness equals about 120 μm.

4. CONCLUSION

The current study has carried out a numerical simulation and an investigation of thermal characteristics of the laser technological process, namely the gas–powder laser cladding. A physicomathematical model of the process and results of the numerical calculations have been presented. Based on analyzing the results of the numerical calculations, continuous and pulse cladding modes have been studied. A possibility is demonstrated of melting metal particles in the laser radiation beam prior to their reaching the surface, which can improve efficiency of the cladding process and upgrade the cladded layer. Some features of the pulse mode of the powdered material cladding have been considered and it has been established, that, in this case, the thickness of the thermal heating zone of the substrate material increases markedly.

REFERENCES

1. V. M. Weerasinghe and W. M. Steen, Laser cladding with blown particles, *Metal Constr.* **19,** 581–585 (1987).
2. A. G. Grigoryantz, *Principles of Laser Treatment of Materials.* Izd. Nauka, Moscow (1989).
3. H. W. Bergmann and R. Kupfer (Editors), *Proceedings of the European Conference of Laser Treatment of Materials.* ECLAT-90, vol. 1, 2, Erlangen., FRG (1990).
4. J. Mazumder and A. Kar, Nonequilibrium processing with lasers, *World Laser Almanac* **1,** 17–24 (1988).
5. F. V. Bunkin, N. A. Kirichenko and B. S. Lukyanchuk, Thermochemical effect of laser radiation, *Uspekhi Fiz. Nauk* **138,** 45–94 (1982).
6. D. S. Bobuchenko, V. K. Pustovalov and I. A. Khorunzhii, Mathematical simulation of a nonlinear propagation of intense optical radiation in a metal aerosol layer, *Matemat. Model,* **2**(6), 26–39 (1990).
7. D. S. Bobuchenko and V. K. Pustovalov, Numerical simulation of gas-powder laser cladding of metal materials onto a substrate, *Matemat. Model.* **3**(3), 109–122 (1991).
8. V. K. Pustovalov and D. S. Bobuchenko, Heating, evaporation and combustion of a solid aerosol particle in a gas exposed to optical radiation, *Int. J. Heat Mass Transfer* **32,** 3–17 (1989).
9. I. K. Kikoin (Editor), *Tables of Physical Quantities.* Reference Book. Atomizdat, Moscow (1976).
10. N. B. Vargaftik, *Reference Book on Thermal Physical Properties of Fluids.* Nauka Press, Moscow (1979).
11. N. Ye. Drits (Editor), *Properties of Elements.* Reference Book. Izd. Metallurgiya, Moscow (1985).
12. S. I. Anisimov, Ya. A. Imas, G. S. Romanov and Yu. V. Khodyko, *Effect of High-Power Radiation on Metals.* Izd. Nauka, Moscow (1970).
13. N. N. Rykalin, A. A. Uglov, I. V. Zuev and A. N. Kokora, *Laser and Electron-Beam Treatment of Materials.* Reference Book. Izd. Mashinostr., Moscow (1985).
14. H. Koebner (Editor), *Industrial Application of Lasers.* Wiley, New York (1984).
15. V. I. Konov and V. N. Tokarev, Temperature dependence of absorptivity of aluminum targets at the wavelength of 10.6 μm, *Kvant. Elektr.* **10,** 327–331 (1983).